

Cavitation Bubble Regimes in Polymers and Viscous Fluids

Rune W. Time and A. H. Rabenjafimanantsoa

University of Stavanger , Norway

ABSTRACT

Cavitation in Newtonian and non-Newtonian fluids may drastically change their rheological properties. One way to induce cavitation is by means of high amplitude acoustic waves. This method also provides better defined pressure fields than with cavitation in shear flows in valves or around rotating bodies like in pumps, mixer impellers or propellers. Cavitation induced bubbles may cause several problems. Typically the impact of bubbles on mixture fluid density and rheological properties may lead to unpredictable flow and pressure gradients. Also the presence of even small amounts of gas bubbles modifies the sound velocity, which may influence the critical Mach number for sonic flow (choking condition) in valves, pumps and even journal bearings. In this work the creation mechanisms and the subsequent bubble movement and stability were investigated. An “acoustic horn” (with a frequency of 24 kHz) was used as source, combined with high-speed video to study bubble dynamics and liquid flow. The experiments indicate unexpected self-amplifying effects over time, both regarding bubble accumulation and wave pressure field attenuation, qualifying for using the term cavitation *regimes*. Chemo-mechanical degradation of fluids due to high pressure amplitudes and shear fields was also investigated as part of the experiments.

INTRODUCTION

High energy acoustics provides methods to investigate cavitation and bubbles in a more controlled way than in flows involving turbulent shear fields or flow acceleration. It is also simpler to monitor than with flows, since tests can be carried out in static cells. Cavitation in Newtonian flows is well known and studied for many decades for applications like ships and submarine hulls, propellers, valves and pumps. Cavitation with polymers and non-newtonian fluids has been less studied but are also of high technological importance. Examples are in machinery journal bearings², petroleum engineering [drilling fluids in pumps and valves], medicine (ultrasonic muscle treatments, blood flow measurement, kidney stone removal, liposuction, medical imaging)

LIQUID CAVITATION MECHANISMS

Cavitation has become a common term for apparent “rupture” of liquids by pressure reduction below the vapour pressure. It is different from boiling in that it usually appears quickly and locally by creation of small bubbles that collapses rapidly when the surrounding pressure normalizes. In the collapse stage high pressure waves are generated which may exceed 1000 bar. They are associated with wide frequency band noise. The local pressure reduction may be

induced in many ways, such as high velocity nozzle flows, choked flows in valves (“jet flows”) or around obstructions in the flow. It can also occur in vortex flows with very high rotational speeds¹⁷. Finally, since the vapour pressure is temperature dependent, cavitation can also be generated by fast local heating induced by powerful lasers, electric sparks, or as here, by strong ultrasonic waves. Cavitation in a flowing liquid (e.g. “jet cavitation”) is normally characterized in terms of the cavitation number

$$Ca = \frac{p - p_v}{\frac{1}{2}\rho u^2} \quad (1)$$

where ρ is density, u is a characteristic flow speed, p is the local pressure and p_v is the vapour pressure of the liquid.

Acoustic cavitation

In acoustic induced cavitation without flow it is the negative pressure amplitude of the acoustic wave which determines whether cavitation may occur. Consequently a modified ultrasonic cavitation number Cu is appropriate as

$$Cu = \frac{p - p_v}{P_0} \quad (2)$$

Here P_0 is the characteristic ultrasonic pressure amplitude. In this work P_0 can be set equal to P_s , the acoustic wave pressure just outside the oscillating surface face of the “acoustic horn” used in the tests. It will be described in the next section. The horn provides pressure pulses with amplitude up to 17 bar, sufficient for strong cavitation. The cavitation number is supplemented by a dynamical theory to describe how bubbles respond to the continuous process of growth, oscillations and collapse during the acoustic wave cycle. The acoustic field also “forces” translational motion of bubbles. The radial oscillatory motion (volume change) of a single bubble due to a time varying pressure field can be modelled with the Rayleigh-Plesset (often referred to as the RPNNP) differential equation^{3,10}.

It involves the liquid density and viscosity, surface tension, vapour pressure and gas polytropic constant. It may be used also to derive the resonance frequency of bubbles which is highly important for the translational motion in an oscillatory pressure field.

We refer equations and derivations to the excellent overviews of acoustic induced cavitation dynamic^{1, 3, 8, 11, 12, 17}.

Translational motion is associated with the so-called primary Bjerknes force which describes motion of a single bubble resonating in an external oscillating field. Bubbles less than resonance size attract towards pressure antinodes, and opposite for larger bubbles. The resonance frequency of the bubbles also determines the secondary Bjerknes force which describes relative motion between two bubbles caused by the mutual radiative pressure and velocity coupling.

Cavitation in polymer solutions has been studied theoretically^{6, 14}, but modelling cavitating bulk fluid volumes with more than two bubbles is theoretically very challenging.

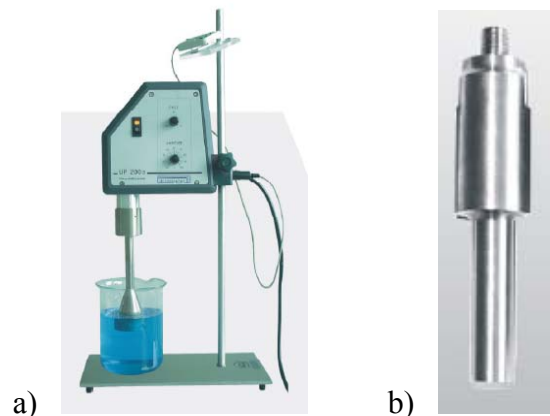


Figure 1a). “Acoustic horn” (picture from the user manual). The submerged cylinder (tip) oscillates with a maximum amplitude of only 125 micrometers.

1b) The shape of the tip H14 (14mm tip face diameter). Tip is submerged 20 mm into the liquid, as seen in several pictures later.

The pressure waves, vortices, interfacial motion and liquid flow create a self-organized geometrical system (“regime”) which is not apparent from straightforward inspection of the governing dynamic equations.

At this stage it will be necessary to gain insight into collective and bulk behaviour from experiments, as in this study. Some experimental works were found in the literature^{5, 7, 14, 16}. However it will still be of importance to study few bubble systems and flow details in addition to larger cavitation clouds.

EXPERIMENTS AND SETUP

The experimental setup is shown in figures 1 and 2. The “acoustic horn” (type UP400S, Hielscher Ultrasound Technology) consists of a piezoelectric amplifier connected to a cylindrical rod (“sonotrode”) acting as a piston that oscillates at high frequency. It was set to induce cavitation in test cells (liquid filled glass cylinders) of volumes 100ml. The cell volume was found not to influence the cavitation pattern provided the distance to the cylinder walls exceed a few centimetres.

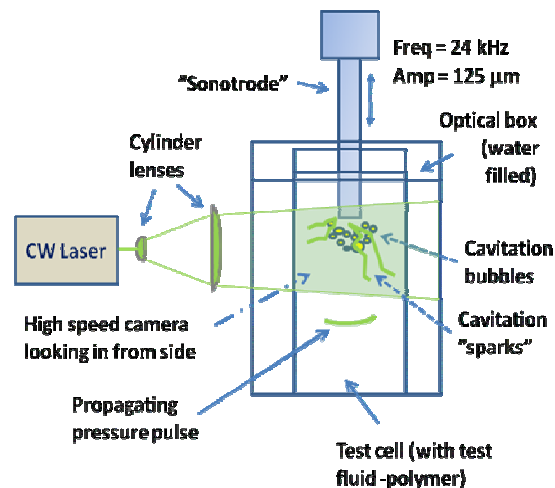


Figure 2. Experimental setup.

The maximum power delivered using the sonotrode “Tip H14” (see Figure 1b) is 105W/cm^2 (according to the manufacturer).

The pressure amplitude of the acoustic wave can be calculated with the expression

$$P_s = (2I\rho_0c_0)^{1/2} \quad (3)$$

Here I is the intensity (maximum with the tip used is 105 W/cm^2). For water the liquid density ρ_0 is 1000 kg/m^3 , with a sound velocity c_0 of 1500m/s . The acoustic horn has a working frequency of 24 kHz , and the amplitude is adjustable to 125 micrometer .

The instrument can be controlled to give from 20% - 100% of maximum piston amplitude, with an inter-pulse period of 1 second . The pulse duty cycle is selectable from 10% (pulse burst length = 100ms) to 100% (continuous) of the pulse period. Using equation (3) we get maximum theoretical pressure amplitudes up to 17.7 bar . Even at only 20% output this is sufficient to create vacuum for a substantial part of the negative going sinusoidal pulse.

The cavitation eruptions are recorded with a high-speed camera (SpeedCam MiniVis e2) that records up to 2500 fps at full resolution 512×512 pixels. It can record up to 120.000 fps at reduced resolution. The camera has onboard memory for 8223 full frames at full resolution. Images are downloaded to computer via a GigaBit Ethernet cable by means of a dedicated communication program (“MotionBlitz”, by Mikrotron).

Illumination is set up with a continuous wave (CW) diode wave (Suwtech) giving a beam with adjustable energy up to 200mW , and fixed 532nm wavelength. The beam was expanded and collimated into a 1mm thick and 5cm wide, nearly parallel “light sheet”, using two cylinder lenses as indicated in figure 2. All pictures seen in the figure therefore essentially show 2D cross sections through the cavitation region.

Thermal effects

The supplied energy from the acoustic horn will cause a small heating of the fluid, with slight thermal modification of the

rheological parameters. In any case these effects were minimized by using short test periods, typically 10 seconds. In most tests only 20% of maximum energy and 10 % duty cycle was used. For a liquid volume of 100 ml water this corresponds to 0.4 degrees Celsius for a test lasting for 10 seconds. Additional stabilization was provided by a water filled external acrylic box which also serves as an optical cell. For oils the heat capacity is typically 4 times higher than for water, so the heating effect was even less.

However the local instantaneous thermal effect can be considerably higher. Sonoluminescence⁴ occurs frequently in cavitation. The maximum temperature during bubble collapse may be higher than 10.000 degrees Kelvin. This gives sufficient energy to induce local phase decompositions and even molecular changes of permanent nature.

Experiments and fluids

Several fluids, both Newtonian and non-Newtonian were used for the tests. Those reported here are; tap water, mineral oil, glycerol (85% in water), “Densept” (a hand disinfection gel), and PAC (Poly Anionic Cellulose, 400ppm in water). Both PAC and Densept were found to follow a traditional power-law model for shear stress fairly well.

$$\tau = K \left(\frac{du}{dy} \right)^n \quad (4)$$

The flow consistency index K and flow behavior index for PAC and Densept is given in figures 13 and 14 before and after tests. Densept is a clear gel containing 70% ethanol, carbomer around 20%, 2% glycerol and the remaining is 2-propanol. It is volatile with a vapour pressure nearly as for alcohol in water at the same concentration (see Table 1).

Experimental recordings

Experiments were recorded and stored both as series of pictures at high frame rates (1000- 2000 fps) and also as shorter high-

speed videos. Altogether 15 experiment series were carried out, each with 3500 – 4000 pictures, and also 20 videos. The information content even in one picture is high. Adding all the pictures makes it a formidable task to interpret.

The videos provide in a condensed way the dynamics of the cavitation patterns. A comparison study of individual pictures or pairs of pictures reveal details on more instantaneous “frozen” time scale. It is fair to say that without the videos (or running fast sequences of pictures) it would be far more difficult to interpret the dynamics properly. Only a few selected aspects can be covered in this short paper.

The cavitation patterns were initially believed to fall into four main categories, following largely the fluids rheological properties. These include; low viscosity Newtonian (water, and mineral oil; 3cP), high viscosity Newtonian (glycerol;109 cP), shear thinning (PAC 400) and gel (Densept).

Water cavitation

Cavitation for all the fluids including water appears with strong similarity to electric “sparks” locally around the edge of the oscillating tip (figure 3), as well as along the jet (figure 4). Note that the colors in the images are inverted for clarity, so dark fields are in the original images shiny or strongly illuminated. A series of other images in this work will reveal patterns of different “topology”.

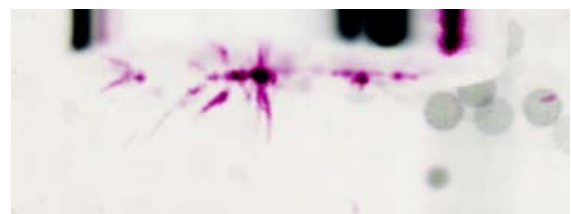
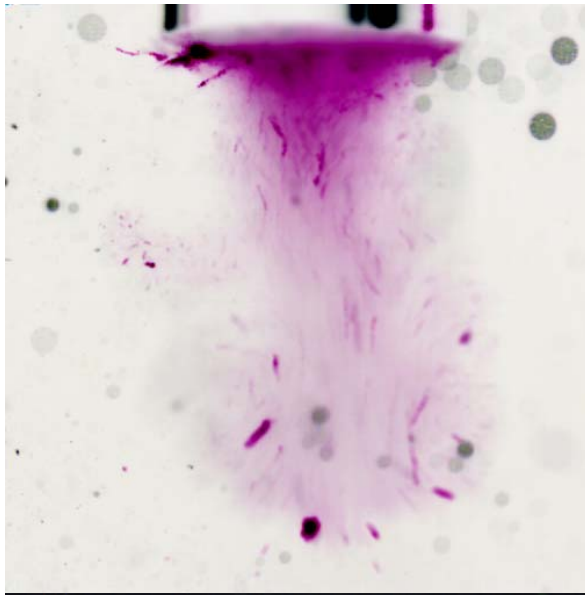


Figure 3. Cavitation starting in water. Close up of initial cavitation sparks radiating from the sonotrode face (seen slightly from below) in water 3.4 ms after start of pulsing. Tip face edge is exaggerated with a grey ellipse



23/03/2011 15:51:05 0706 0603.0[ms] 512x510, 1169 Hz, MotionBLITZ
MiniVis #00164, V1.9.0
Pure water - acoustic horn cavitation lowest energy [20] - Zeiss lens - 44cm
distance

Figure 4. Typical cavitation pattern in water 24.4 ms after start of pulsing. Colors have been inverted for clarity (light = originally dark, dark = originally shiny). The central jet and the rolling torus in its front are clearly defined.

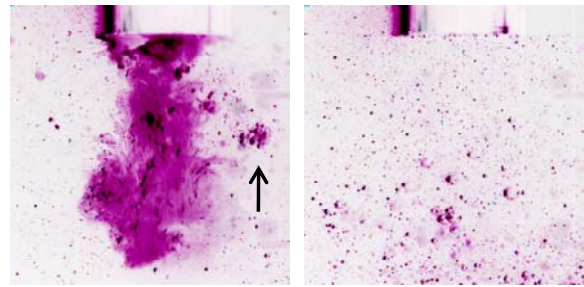
Other researchers¹⁴ use analogous names as we do here, e.g. ALF (Acoustic Lichtenberg Figures) associated with the typical fractal branching patterns of electric sparks.

In water, the cavitation develops quickly into an axial jet with a micro-bubble cloud and some fairly large cavitation bubbles (radius > 100 micrometer) ejected along the jet axis. This is demonstrated in figure 4.

The bubble patterns in water vary from pulse to pulse, except for a repeating presence of the initial streaming giving a flow momentum in the jet direction.

Mineral oil cavitation

Tests with mineral oil showed similar behaviour as water, with pronounced jet production. In mineral oil there was also more vigorous bubble production and excitation, nearly “explosive” in appearance, as seen in figure 5. Out-gassing of lighter volatile hydrocarbons created permanent



a) Frame 3416,
t = 2753.7 ms

b) Frame 3941,
t = 3177.1 ms

Figure 5. Cavitation in mineral oil shows vigorous bubble creation and deformation. Arrow in a) points at a strongly oscillating and fingering bubble which was dispersed after a few milliseconds.

b) shows numerous scattered bubbles 110 milliseconds after stop of pulsing.

bubbles with diameter up to 3 millimeter. These bubbles participated in the subsequent pulses.

Glycerol cavitation

Examples of cavitation in glycerol are shown in figures 6 - 8. It appears to be quite different from water. It exhibits a distinct time development during each pulse. In the tests with glycerol each pulse lasted for 235 milliseconds. The patterns also develop from pulse to pulse. Figure 6 shows the development in glycerol for the first 25 milliseconds of a single test from pulse start in a) with $\Delta t=0$ to the last picture f).

An air bubble was initially placed under the tip face for visualization of the velocity and pressure field. The bubble undergoes several “near destruction” stages, but recovers after ejecting smaller bubble fragments.

Image c) in figure 6, shows how initial cavitation “sparks” appear as closed rolls or spirals, before expanding and releases into the fluid. Figure 7 shows a close-up of the bubble marked in figure 6e), and will be commented later under single bubble regimes.

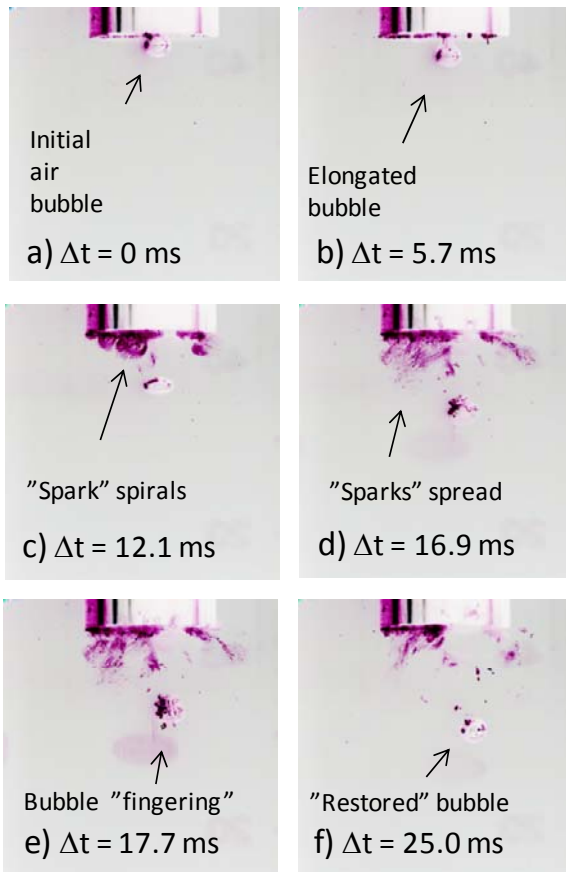


Figure 6. Development of cavitation in glycerol 85% during the first 25 ms after start of pulse one.

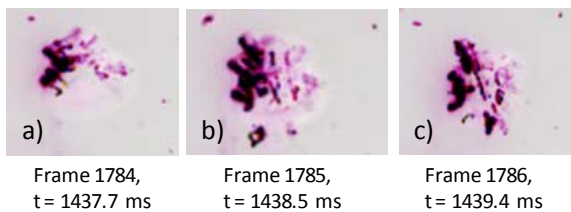


Figure 7. Close up of the bubble fingering in figure 6e), revealing a very complex pressure wave pattern, at times spiralling around the bubble.

The cavitation pattern in glycerol is apparently much more confined around the sonotrode tip than for water. A sequence of pulses at later stages is shown in the series of pictures in figure 8. Each frame in figure 8 is taken 217 ms after the pulsing has started (“stroboscopic display”). After this stage of development the cavitation exhibits a semi steady coronal

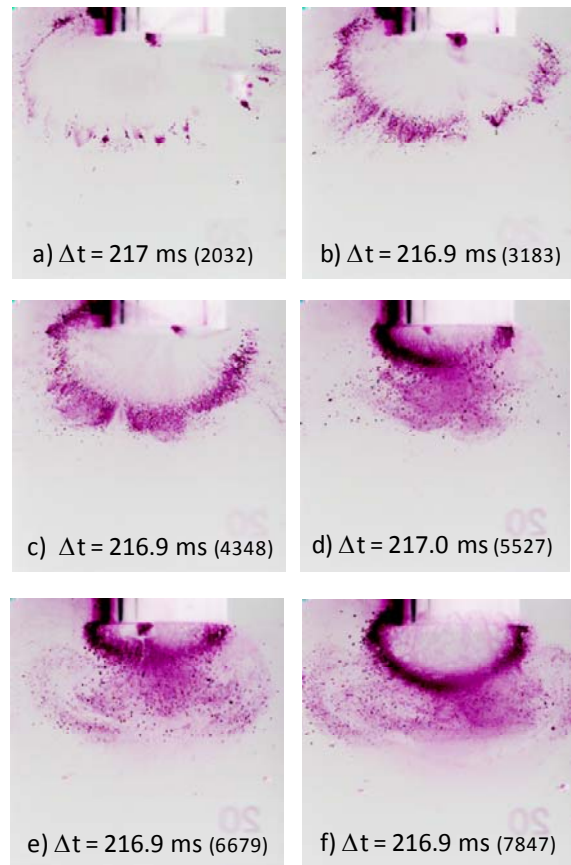


Figure 8. “Stroboscopic” images of cavitation showers in glycerol, recorded 217 ms (+/- 0.1ms) after start of 6 consecutive pulsing periods (at 1 second intervals). Frame numbers in parenthesis. Image a) is for the first (“virgin”) pulse.

ellipsoidal pattern (“bubble shell”) around the tip face, but shooting out frequent “jets” through the bubble shell.

Densept cavitation

Cavitation in “Densept” fluid shows a quite different dynamics. The acoustic “sparks” emerge quickly (starting after 6 ms), and the subsequent propagation of the cavitation pattern is much more complex, but also more localised than for the Newtonian fluids.

In figure 9 is shown a series of pictures where cavitation bubbles are captured and dragged along “sparks”, with striking resemblance to solar mass ejections

following closed magnetic field lines. The “bigger” cavitation bubbles marked in the figure move counter-current with apparent the movement of the very small bubbles that constitute the “field lines”.

Figure 10 shows the “relaxed” cavitation patterns just after each pulse burst has stopped. During the first 7 sequences it seems that the cavitation region is nearly unchanged. This is just apparent. After continuous “treatment” the behaviour is as shown in figure 11. This is similar to what is seen for water. The mechanism is however very different; after 50-60 pulsings (over 1 minute in total) a low viscosity “tunnel” is created in the gel. In this tunnel the fluid now appears low viscous, and the jet formed is confined within this tunnel.

Over longer time the gel will degrade over the whole cell volume. It was observed after a period of several days that the gel partly reforms, but has now much lower resistance to shear force breakdown. The Densept gel is composed of carbomer (Carbopol 980) dissolved in alcohol. The viscometer analysis of Densept gel shows that it follows essentially a power law model. The gel behaviour is a result of uncoiling of the polymer due to the formation of hydrogen bonds or electrostatic interaction⁹ and does not involve other cross-linkers that would introduce yield-point.

PAC cavitation

Also a polymer, PAC was believed to behave more like Densept. However the jet streaming in PAC was more like in water, except for strong suppression of larger streaming cavitation bubbles. It was necessary to increase the acoustic power three times to get similar behaviour as in water. Most likely this is a viscosity effect. Densept which has even higher overall viscosity also produced mainly microscopic bubbles. Similar to Densept a characteristic seen in PAC was distinct cavitation “arcs” connecting the sonotrode side and face.

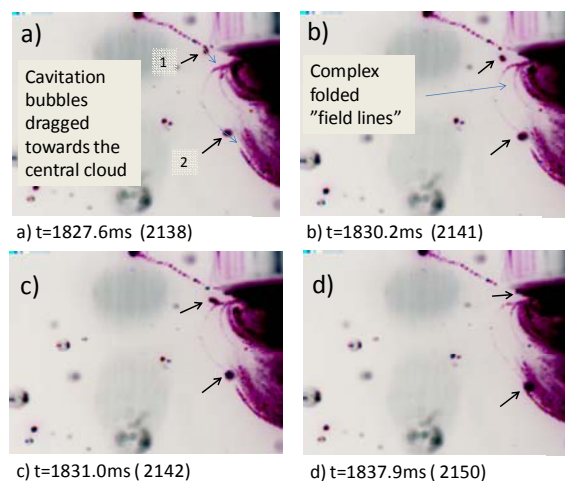


Figure 9. Motion of single bubbles in Densept. Bubbles marked 1 and 2 are dragged towards the center of the cavitation jet, while much smaller bubbles in the “field lines” move in opposite direction. The start of the pulsing was at $t = 1784\text{ms}$, 42ms before image a). Frame numbers in parenthesis.

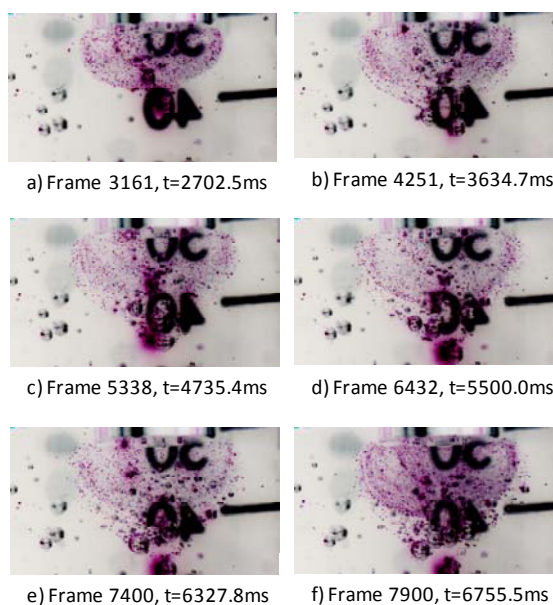


Figure 10. Stoscopic sequence of “fossile” cavitation patterns in Densept. Each image is 800 ms after pulse stop. Notice that the surroundings are only slightly affected after pulse stop. (Numbers in the background stem from the test cylinder cell wall)

This made it easier to identify possible mechanism for the vortex formation in acoustic cavitation as described in the figures 12.

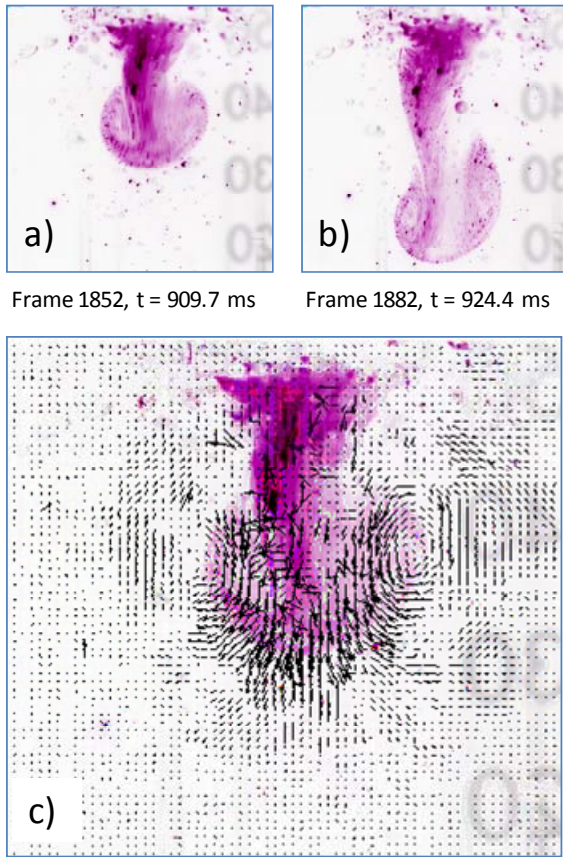


Figure 11. Cavitation jet in Densept after longer “sonication”; exposed to 5 series of 15 pulses (=75). The pattern in a) and b) now resembles low viscosity Newtonian behaviour. c) PIV analysis (MatPIV¹⁸) of picture a) showing the velocity vectors in the jet and in the recirculation pattern of the torus.

CAVITATION “REGIMES”

The experiments indicate that one may discriminate between at least three different length scale mechanisms, each exhibiting flow regimes. These are; i) single bubble regimes ii) vortex bubble regimes, and iii) overall regimes.

Overall regimes

Starting with iii) the overall regimes, fluid rheological parameters cannot alone explain all the observed cavitation patterns. As an example; glycerol is in itself a Newtonian fluid. But seeded with cavitation micro-bubbles the dynamical response is modified. The mixture density decreases, and compressibility increases.

The acoustic wave speed normally decreases with increasing gas fraction. Consequently the acoustic impedance becomes position dependent, being associated with the local gas fraction. The acoustic waves now traverse a strongly non-homogeneous, non-isotropic medium. The acoustic energy density and pressure (per unit fluid volume) increases as the sound speed decreases (“Tsunami rise” effect), and this self-amplifies the cavitation locally. It also partly sets up a damped acoustic resonator condition outside the tip face under conditions as shown in figure 5. It may also be seen in figure 8 that the ellipsoidal shock front contracts from one pulse sequence to the next for the first 5 pulses. It seems to expand in the last image f), but the video suggests this could be due to inertial drifting of the cavitation bubble cloud.

The recorded videos reveal a much richer dynamics than can be seen by just considering still pictures, since the dynamics and time evolution is very important. They indicate that the shock front behaves like an elastic “shell”. It is occasionally penetrated by acoustic bursts from the tip face, pushing older bubbles further away from the acoustic horn. Once the shell breaks, it allows also other bubbles to escape from the interior. The regime could be likened with a “pressure boiler relief”. Perhaps this occurs with some frequency, but longer time series are needed to see if this really is cyclic. One problem for such testing however is the acoustic heating.

The effect of rheology is obviously not only connected to “class”. Although Densept and PAC both are shear thinning fluids they did not show the same time development. For the first pulsing period in Densept the acoustic wave penetrated only a short distance into the fluid, creating a large amount of micro-bubbles. When the pulse stops, these bubbles remain, due to the high effective fluid viscosity. And for the same reason as with glycerol when a new pulse

sequence start the energy is confined to a small region outside the tip.

The large energy deposited partly decomposes the gel, consisting of alcohol and a carbomer. Decomposition perhaps also takes place on a molecular basis and the viscosity drops markedly in the confined cavitation region. Thus as more and more pulses are emitted, a pocket of lower viscosity fluid is created. The wave now causes streaming and recirculation inside the bag. However, there is substantial shear between the recirculating fluid and the surrounding gel. This causes the bag to expand gradually over time as more and more pulses are injected into the fluid. It seems adequate to characterize this as a “wormhole” regime.

PAC, also a shear thinning fluid behaves more similar to water than to Densept. A significant jet is propagating forward through the cell. The main difference from water was lower population of large distinct bubbles. Appearing as a diffuse cloud pattern the bubbles could be in the sub micrometer regime, with small eruption of aggregates of 10-100 μm bubbles.

Finally, glycerol being a Newtonian fluid produced patterns more similar to Densept. The main feature was the confining “shell” around the horn tip. It was frequently penetrated by spurious jets allowing other bubbles to escape. Compared to Densept this pattern was fairly stable, while Densept was degraded and developed a widening cavitation tunnel over time.

Vortices - origin of cavitation “sparks”

Cavitation sparks are often explained as “fracturing” liquid. They emerge both from the horns sides and face. Sparks from the sides seem to connect towards the fluid jet, merging with jet and emit downwards. Another plausible “spark” mechanism is creation of strong vortices that attach to stagnation points on the cylinder side wall. These vortices are created by the oscillating up and down fluid movement in the wall

boundary layer, and might be compared with tip cavitation on wing profiles. The vortex centre is an extreme low pressure zone where cavitation micro bubbles are generated and captured by the intense centripetal forces. In that way they may, if present, also serve as visualization particles of the low pressure field. There are also transport mechanisms along the vortex lines that could be associated with the pumping mechanism of the Bjerknes forces. In figure 12 is given a sketch and images from cavitation in PAC 400 ppm to illustrate the physics.

Merging of smaller bubbles

Several recorded images show small bubbles in the bulk fluid distant from the jet, suddenly starting to move quickly and merging as if dragged together by invisible elastic strings. In one such “event” with PAC 400 five bubbles merged into one in just 15 ms. Explaining this in terms of the second Bjerknes force seems plausible, but not provable in lack of detailed pressure field visualization.

Single bubble regimes

“Single bubble regimes” classify their oscillatory response to the external flow and pressure field. In figure 6 is shown a series of close-up images of a single 3mm diameter air bubble. Depending on the saturation of nitrogen and oxygen in the water, the air bubbles will mainly oscillate and eventually fragment into smaller bubbles. The presence of air will therefore attenuate pressure amplitudes, but may on the other hand induce more sonoluminescence. These mechanisms are associated with the effective pressure in the bubbles, which are given as¹¹

$$p_{\text{eff}} = p_0 + \frac{2\sigma}{R_0} - p_v \quad (5)$$

Here p_0 is the surrounding hydrostatic pressure, σ is the surface tension, R_0 is the equilibrium bubble radius, and p_v is the

vapour pressure of the fluid. For a mixture of gases the vapour pressure follows Raoult's law (assumed equilibrium thermodynamics). Some data are given¹⁰ in Tables 1 and 2. Generally the surface tension, density and viscosity are all important for the oscillation and breakup mechanisms.

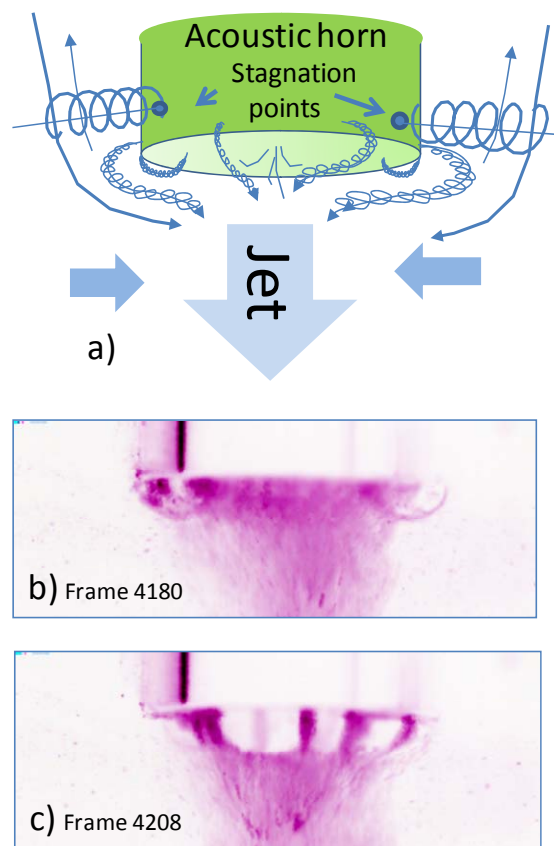


Figure 12. a) The cavitation vortices (“sparks”) arise as a result of strong shear along and in towards the axis of acoustic horn. The pressure at the center of the vortices is close to the vapour pressure of the liquid. PAC images b and c) Vortex lines during the active pulsing emerging from the horn side. c) Immediately after the pulse burst stops, vortex lines are still attached to the edges of the cylinder face, connecting to the tail of the jet.

Micro-bubbles associated with the fluid cavitation, with diameters down to 10^{-7} m, are theoretically spherical. However, being that small, the surrounding boundary layer is larger than the bubble itself. Consequently the description of interface mass transfer

rate and non-equilibrium thermodynamics becomes very complex. Their dynamical behaviour is still mainly accessible via molecular dynamics or Lattice-Boltzmann simulation.

Table 1: Vapor pressure of relevant fluids.

Fluid	Vapor pressure (kPa, at 20 °C)
Water	2.3
Ethanol	5.95
2-Propanol	2.70
Glycerol	$3.3 \cdot 10^{-4}$ (at 50 °C)
Densept	5.85 (mainly ethanol)

Table 2: Surface tension of relevant fluids [8]

Fluid	Surface tension (mNm^{-1} , at 20 °C)
Water	72.86
Ethanol	22.39
2-Propanol	21.3
Glycerol	64
Densept	Not measured or relevant

Impact on polymers rheology

Sonication may impact on rheology¹⁵ in various ways. In figures 13 and 14 is shown the rheology of Densept and PAC respectively before and after a 60 second exposure to “sonication”. The analysis was done with a Physica UDS 200 rheometer with cone plate configuration.

The viscosity is clearly reduced, but the mechanisms are probably different for the two fluids. The recorded images for PAC experiments did not exhibit the same development of a “cavitation tunnel”, and the bubbles produced were so small that they disappeared some milliseconds after stopping the pulse.

The change seen for Densept was more likely due to alcohol-gel separation, and perhaps polymer degradation in the cavitation tunnel. The fluid in the cavitation tunnel could easily be poured out of the test cell, and had a stronger smell of alcohol than the original gel before testing.

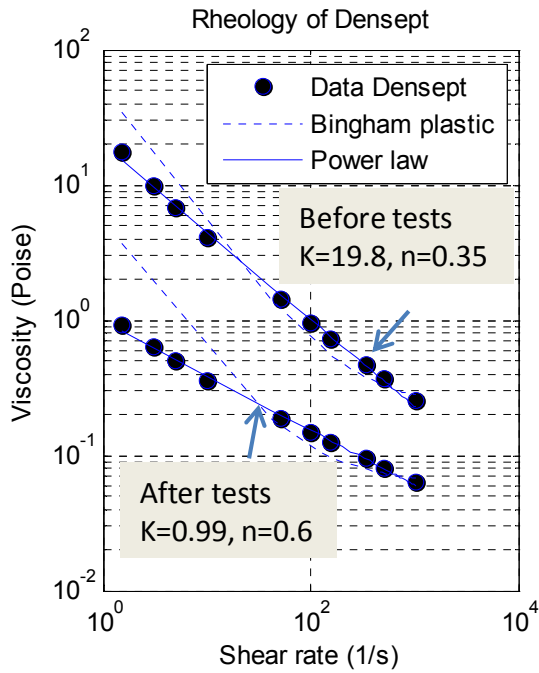


Figure 13. Rheology of Denssept before and after sonication tests. Denssept behaves essentially as a power-law fluid. K and n as defined in equation 4.

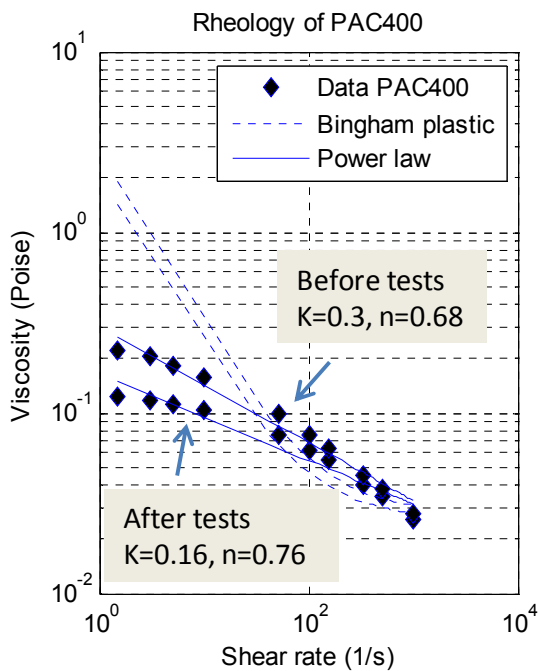


Figure 13. Rheology of PAC 400 before and after sonication. K and n as defined in equation 4.

A chemical analysis will be a necessary future task to determine the physical and chemical changes during sonication.

Generally one should classify single bubbles according whether they are weakly cavitating (low amplitude) or strongly cavitating with sonoluminescence¹². In the latter case chemical reactions are likely and should influence rheology even more.

CONCLUSIONS

The experiments with cavitation in Newtonian and non-Newtonian fluids using acoustics showed a comprehensive range of phenomena, giving rise to a challenging task of classification. There clearly are such classes, or flow-regimes. But the “flow regime map” is multi-dimensional, and does not follow a straight forward scheme based only on rheology class. The reason seems to be a complex interplay of hydrodynamics involving vortex formation and boundary layers, cavitation thermodynamics, and the complex acoustic pressure field. This is completed by the interaction of the bubble oscillations with the acoustic waves, described for the simplest cases with the primary Bjerknes forces. However, in large bulk volumes a self-organized pattern is set up in which the medium establishes heterogeneous pattern according to local acoustic wave velocity and impedance. The stability of these patterns regulates both the local and global patterns as well as the time development.

Improved understanding of acoustic cavitation in non-Newtonian fluids obviously depends on the development of both theory (“time dependent rheology” involving strong gradients and phase transition), as well as much higher resolution in time and space of instrumentation. This could open up for developing cavitation technology of fluids into a “nano-hydrodynamic” technology, with a wide range of applications.

ACKNOWLEDGEMENT

The instrumentation for this work, laser and high-speed camera was granted from the Norwegian Research Council.

REFERENCES

1. Ashokkumar, M., “The characterization of acoustic cavitation bubbles – An overview”, *Ultrasonics Sonochemistry*, 18 (2011) 864–872
2. Berker: “Effect of polymer on flow in journal bearings”, *J. Non-Newtonian Fluid Mech*, Volume 56, Issue 3, March 1995, pp. 333-347
3. Brennen, C. E.: “Cavitation and Bubble Dynamics”. Oxford University Press, New York, 1995
4. Brenner, M.P., Hilgenfeldt, S., Lohse D. “Single-bubble sonoluminescence”, *Rev. Mod. Phys.* 74, pp 425–484 (2002) :
5. Brown, S.W.J et al – “An experimental study of liquid jets formed by bubble-shock wave interaction”, *Exp in Fluids* 29 (2000) pp. 56-65
6. Brujan, E.A. : “The Effect of Polymer Additives on the Bubble Behaviour and Impulse Pressure”, *Chem. Eng Science*, Volume 48, Issue 20, Oct 1993, pp. 3519-3527.
7. Divoux, T. et al: “Acoustic emission associated with the bursting of a gas bubble at the free surface of a non-viscous fluid”, *Physical Re E Stat Nonlin and Soft Mat Phys* 77 (2008)
8. Doinikov, AA.: “Influence of neighboring bubbles on the primary bjerknes force acting on a small cavitation bubble in a strong acoustic field”, *Phys Rev E Stat Phys Plasmas Fluids Relat Interdiscip Topics*. 2000 Nov; 62(5 Pt B):7516-9
9. Islam, M. T. et al.: “Fourier Transform Infrared Spectroscopy for the Analysis of Neutralizer-Carbomer and Surfactant-Carbomer Interactions in Aqueous, Hydroalcoholic, and Anhydrous Gel Formulations”, *The AAPS Journal* 2004; 6 (4) Article 3
10. Jasper, J. J., *J. Phys. Chem. Ref. Data*, 1, 841, 1972.
11. Leighton, T.G. et al: “Primary Bjerknes forces”, *Eur. J. Phys.* 11 (1990), pp. 47-40.
12. Margulis M.A.: “Sonochemistry and Cavitation”, Gordon and Breach Publ, 1995
13. Marston, J.O. et al: “Cavitation structures formed during the rebound of a sphere from a wetted surface”, *Exp Fluids* (2011) 50:729–746
14. Mettin, R. Luther, S. Ohl, C.D and Lauterborn, W.: “Acoustic cavitation structures and simulations by a particle model”, *Ultrason Sonochem.* 1999 March; 6(1-2):25-9.
15. Mohod, A.V and Gogate, P.R.: “Ultrasonic degradation of polymers: Effect of operating parameters and intensification using additives for carboxymethyl cellulose (CMC) and polyvinyl alcohol (PVA)”, *Ultrason Sonochem* 18 (2011) 727–734
16. Rabenjafimanantsoa, H. A, Wrobel, B. M. and Time, R. W.: “PIV Visualization of Acoustic Streaming in Non-Newtonian Fluid”, *Ann. Trans. of the Nordic Rheological Society*, Vol. 17, 2009.
17. Siginer, D.A, DeKee, D., Chhabra, R.P.: “Advances in the Flow and Rheology of non-Newtonian Fluids – Part A”, Elsevier, 1999
18. Sveen, J.K.: “MatPIV”, Department of Mathematics, University of Oslo, (2004).